

New PPAR α / γ / δ Optimal Activator Rationally Designed by Computational Methods

Elias C. Padilha,^{a,b} Rodolfo B. Serafim,^{b,c} Deisy Y. R. Sarmiento,^{b,d} César F. Santos,^e
Cleydson B. R. Santos^{*,b,e} and Carlos H. T. P. Silva^b

^aDepartamento de Princípios Ativos Naturais e Toxicologia, Faculdade de Ciências Farmacêuticas,
Universidade Estadual Paulista, Araraquara, Rodovia Araraquara-Jaú km 1,
14801-902 Araraquara-SP, Brazil

^bDepartamento de Ciências Farmacêuticas, Faculdade de Ciências Farmacêuticas de Ribeirão
Preto, Universidade de São Paulo, Av. Prof. do Café, Monte Alegre,
14040-903 Ribeirão Preto-SP, Brazil

^cDepartamento de Biologia Celular e Molecular e Bioagentes Patogênicos and ^dDepartamento de
Bioquímica e Imunologia, Faculdade de Medicina de Ribeirão Preto, Universidade de São Paulo,
Av. Bandeirantes, 3900, Monte Alegre, 14049-900 Ribeirão Preto-SP, Brazil

^eLaboratório de Modelagem e Química Computational, Departamento de Ciências Biológicas,
Universidade Federal do Amapá, Rod. Juscelino Kubitschek, km 02, Jardim Marco Zero,
68902-280 Macapá-AP, Brazil

The peroxisome proliferator-activated receptor gamma (PPAR γ) is a nuclear receptor that acts as a transcription factor, regulating glucose, lipid and inflammation signaling and it is exploited in type 2 diabetes treatment. However, the selective activation of this PPAR subtype has been linked to important adverse effects which can be mitigated through concomitant activation of PPAR α and PPAR δ . In this study, we proposed new PPAR γ agonists using PharmaGist Server for pharmacophore prediction, the molecular docking was performed by GOLD (genetic optimization for ligand docking) v2.2, AutoDock 4.2 and AutoDock Vina 1.1 and QikProp v4.0 and Derek for absorption, distribution, metabolism, excretion and toxicity (ADMET) assessment. One molecule showed high predicted affinity to PPAR γ and favorable pharmacokinetic and toxicity properties. It was then evaluated against PPAR α and PPAR δ and showed greater affinity to these receptors than the controls. Therefore this molecule is a promising drug lead for the development of derivatives and for the treatment of metabolic syndrome with the benefits of a PPAR pan activation.

Keywords: type 2 diabetes, PPAR pan agonist, molecular modeling, ADMET prediction

Introduction

The general cause of mortality among type 2 diabetes mellitus patients is due to dyslipidemia leading to cardiovascular complications. Currently, the drugs used to control these disorders act separately either on reducing blood glucose or lowering triglyceride levels, free fatty acid and low-density lipoprotein. However, the increasing number of cases of patients with diabetic metabolic syndrome requires the development of therapies that act simultaneously reducing glycidic and lipidic levels in a combined effort to ease cardiovascular disorders.¹ Peroxisome proliferator-

activated receptors (PPARs) are nuclear receptors that act as transcription factors, regulating glucose homeostasis, lipid metabolism and inflammation signaling, making them attractive targets for the development of new therapies for metabolic syndromes. They regulate the expression of target genes after forming a heterodimer with 9-*cis*-retinoic acid receptor (RXR) and bind to the peroxisome proliferators response elements (PPRE) in the regulatory region of the target gene. The increased transcriptional rates of their target genes may be increased after interaction with an agonist ligand which alters the conformation of PPAR, exposing the DNA (deoxyribonucleic acid) binding site. Three distinct receptors have already been described, PPAR α , PPAR δ and PPAR γ .²

*e-mail: breno@unifap.br

PPAR γ plays an important role in the regulation of glucose and lipid metabolism and it is widely distributed in adipose tissue.^{3,4} In adipocytes, the PPAR γ activity regulates the expression of genes involved in lipid metabolism,⁵⁻⁷ in addition to the control of the expression of proteins involved in the uptake of lipids by adipocytes.⁸ The PPAR γ activation in adipose tissue presents an indirect activity in tissues which respond to insulin.⁹ This effect was demonstrated using the drug rosiglitazone, a known PPAR γ activator, in an experiment that showed that the drug is capable of increasing the insulin sensitivity of mice with severe insulin resistance but had no effect in mice with absence of adipose tissue.¹⁰

Thiazolidinediones are PPAR γ agonist drugs used for treatment of patients with type 2 diabetes mellitus. Thiazolidinediones can modulate gene expression that increases insulin sensitivity in peripheral tissues causing a reduction in blood glucose.¹¹ In the United States market, three thiazolidinediones, troglitazone, pioglitazone and rosiglitazone, were introduced. Troglitazone presented dangerous hepatotoxicity profile and was removed from the market. Whereas pioglitazone and rosiglitazone are still marketed, however, recent studies indicated that rosiglitazone is associated with body weight gain, increased risk of myocardial infarction and death from cardiovascular causes.¹²⁻¹⁴ These adverse effects are related to the selective activation of PPAR γ . The literature also presents results of drugs that are able to activate concomitantly PPAR α , PPAR β/δ and PPAR γ , this combined activation was able to avoid the adverse effects caused by the PPAR γ selective activation.¹⁵

PPAR α is present mainly in muscle, heart and liver and play a role in hepatic lipid and lipoprotein metabolism. PPAR α agonist drugs, the fibrates, are used as hypolipidemic agents. PPAR δ is widely distributed throughout the tissues¹⁶ and their activation is related in overall energy regulation and fatty acid oxidation, and is able to increase high-density lipoprotein cholesterol levels in diabetic mice and obese rhesus monkeys models.¹⁷ PPAR δ selective agonists can reduce weight gain in mice¹⁸ and may counteract the effects of selective PPAR γ activation.

Drugs, which activate all three PPAR subtypes, cause effects in different tissues at the same time, and are able to control blood glucose levels by increasing glucose metabolism, and also control dyslipidemia, reducing the concentration of triglyceride, free fatty acid, low-density lipoprotein and increase the concentration of high-density lipoprotein in the blood. These effects also prevents the formation of atherosclerotic plaques and therefore reduces cardiovascular risks.^{14,19} Moreover, the effects associated with selective activation of PPAR γ , such as the weight gain,

are not observed.²⁰ Some PPAR pan agonists have entered clinical trials and show a promising field of research in the development of new drugs to treat metabolic syndrome.²¹⁻²³

In this study, we aimed to propose new drug candidates for the treatment of the metabolic syndrome originated from type 2 diabetes. For that, we studied available PPAR γ ligands in order to determine their pharmacophore groups through PharmaGist Server. Then, we made docking studies of PPAR γ binding pocket using the software GOLD (genetic optimization for ligand docking) v2.2 to determine its binding mode with known ligands. From this study, we proposed new molecules that can activate PPAR γ . The interaction of our proposals with PPAR γ was also assessed with AutoDock 4.2 and AutoDock Vina 1.1.2. Thus, we predicted pharmacokinetic and toxicity properties of the new proposes with QikProp v4.0 software and Derek software for Windows v10.0.2. The molecules with higher docking scores were also docked against PPAR α and PPAR δ in order to evaluate the PPAR pan agonism.

Experimental

Selection of protein structure and ligands

The structure of the heterodimer RXR α /PPAR γ , PPAR α and PPAR δ resolved by X-ray diffraction was downloaded from the Protein Data Bank with PDB codes 1RDT,²⁴ 4BCR^{25,26} and 3OZO,²⁷ with resolution of 2.4; 2.5 and 3.0 Å, respectively. The ligands were downloaded at Binding DB server, their CID are: 18944089, 446642, 9843045, 10578809, 77999, 10433070, 44383664, 10004390, 44385396, 10068664, 9827261, 44419783, 11464352, 447458, 44345164, structures of each ligand is displayed in Figure 1 and their physicochemical properties are shown in Supplementary Information section, see Table S1.

The ligands and protein structure for pharmacophore prediction and docking were prepared using the softwares Discovery Studio 4.1 and DS Viewer Pro 6.0, removing RXR α domain and the water molecules. The ligands for docking validations were downloaded with the proteins crystal structures. The agonists controls of PPAR γ , PPAR α and PPAR δ were rosiglitazone (CID 77999), tesaglitazar (PDB 117I)²⁸ and TIPP204 (PDB 2ZNP),²⁹ respectively.¹⁵

Pharmacophore prediction

Fifteen known ligands of PPAR γ were chosen in order to assess what these molecules have in common that allow their binding to the receptor, the pharmacophoric groups and features. We chose these ligands based on their affinity constants (Ki) that ranged from 0.4 to 100

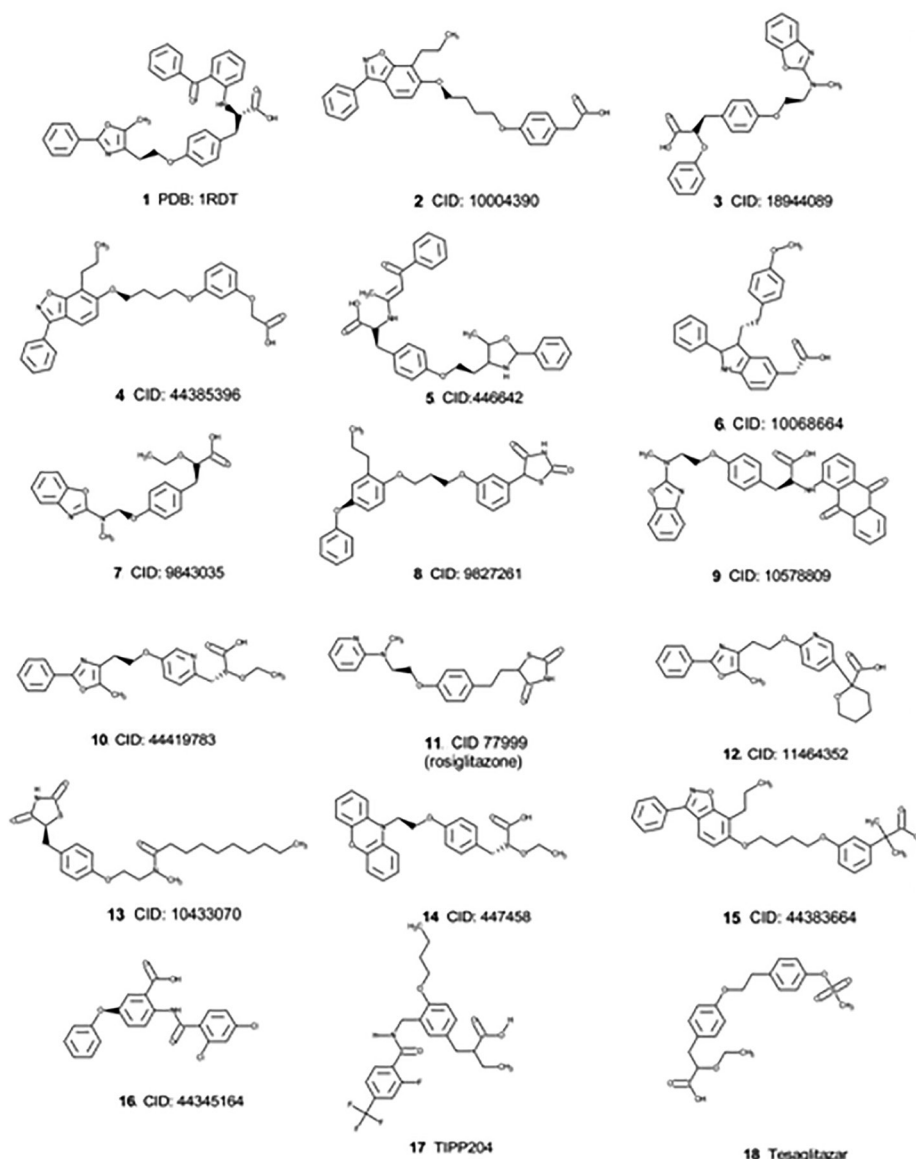


Figure 1. PPAR γ ligands selected. PC CID code was described. The first molecule can be found in PPAR γ receptor crystallography and was the pivot molecule for docking and pharmacophore studies.

and were submitted to the PharmaGist server analysis that determined those features.

Docking study with GOLD

The docking of the Binding DB ligands and our proposed molecules was performed by GOLD software (version 2.2) with default parameters. The population size was 100, selection-pressure 1.1, the number of operations was 10,000, the number of islands was 1, the niche size was 2, operator weights for migrate was 0, mutate was 100, and crossover was 100. The coordinates X = 8.2731, Y = 33.1955 and Z = 7.9396 from the pocket of interest was chosen based on interactions between the amino acids and the pharmacophore predicted, and a 10 Å radius sphere

was defined. Ten solutions were calculated for each ligand and the GOLD score was analyzed.

Docking study with AutoDock 4.2/Vina 1.1.2 and PyRx 0.8

For docking studies among subtypes of PPAR, their specific ligands and proposal molecules, we used the software AutoDock 4.2/Vina 1.1.2 and PyRx 0.8.³⁰ Specific ligands and proposed molecules were optimized in PyRx. The coordinates for PPAR γ was X = 8.2731, Y = 33.1955 and Z = 7.9396, for PPAR α was X = -18.9740, Y = -3.8990 and Z = 46.1490 and for PPAR δ was X = -0.6700, Y = -12.2640 and Z = 48.0570. The coordinates were chosen according to the interaction between the PPAR and its standard agonists.

The energy score function was used to assess the binding free energy of interactions between protein and ligand.³⁰ A visual analysis of the poses was also taken into account for the selection of the best free binding energy. Interactions of ligands and receptor were performed in Discovery Studio 4.1 with default parameters.

Absorption, distribution, metabolism, excretion and toxicity (ADMET) predictions

The pharmacokinetic features of the new proposed molecules were evaluated using QikProp v4.0 software. The range considered acceptable for the different parameters comprises 95% of the drugs. For the prediction of toxicity, Derek software for Windows v10.0.2 was used. The programs were used with default parameters. The combination of the softwares can predict important properties such as absorption, distribution, metabolism, excretion and toxicity groups that constitute the structures of the molecules.

Results

Pharmacophore prediction of PPAR γ ligands

The known ligands of PPAR γ were chosen from the Binding DB web server and selected in a range of affinity constant (K_i) from 0.4 to 100 in order to provide structural variety that can support and validate the methods hereby employed to propose new ligands for this nuclear receptor. Then, all molecules were submitted to the PharmaGist web server in order to determine which chemical groups that these molecules have in common and are responsible for the biological interaction with the receptor.

Twelve out of the sixteen test molecules presented what the PharmaGist identified as the pharmacophoric group with a score of 29.047 (Figure 2). The pivot molecule chosen

for the PharmaGist input was the crystallographic molecule 1RDT, its outputs shown in Figure 2a. The pharmacophoric group is composed of a lipophilic ring followed by another lipophilic group (blue) containing a hydrogen acceptor (green) (Figure 2). We also observed, in the superposition of the test ligands using DS Visualizer 4.1, spatial features comprising angles that most of the test molecules formed between the pharmacophoric group (Figure 2b) and the side chain.

Docking studies of PPAR γ and selective ligands

In order to validate the docking method, the molecule with crystallographic information was submitted to docking until the folding found by the software was similar to the crystallographic information. The best result can be seen in Figure 3a. The primary interaction sites are around the alpha helix between the amino acids residues 278 and 294 which is where the crystallographic molecule is fold around, the docking method identified a conformation that allows the molecule also to interact with a loop between the amino acids 339 and 349. Some interactions may also take place in the helix between 333 and 323. The validation was accepted despite the minor deviation due to the fact that both crystallographic poses are possible and the pose found does not invalidate the other.

The PPAR γ ligands selected in Binding DB presented interactions around the same alpha helix as the crystallographic molecule. They also presented overlapping of the predicted pharmacophore groups indicating that in fact these groups are important for the interaction with the protein. Importantly, the twist of the molecules observed in the prediction of pharmacophore was observed in the docking, indicating that it is also relevant for interaction (Figure 3b). Therefore, both the pharmacophore groups and the angulation of the molecule will be preserved for the development of new activators of PPAR γ .

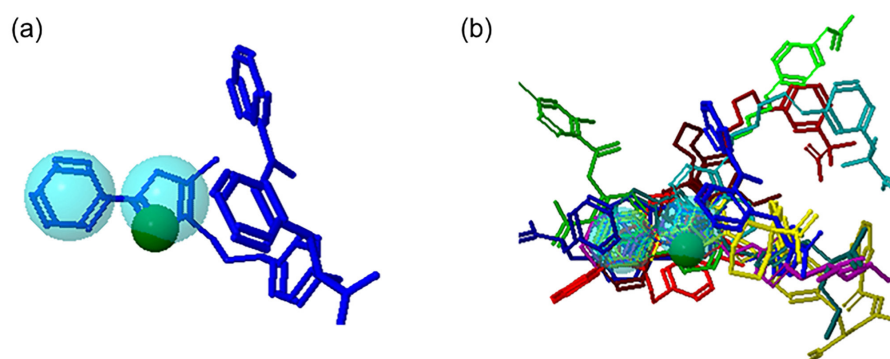


Figure 2. PharmaGist superposition of the test molecules based on its pharmacophoric site. Blue spheres represents lipophilic rings and green sphere show a hydrogen acceptor from pharmacophoric group.

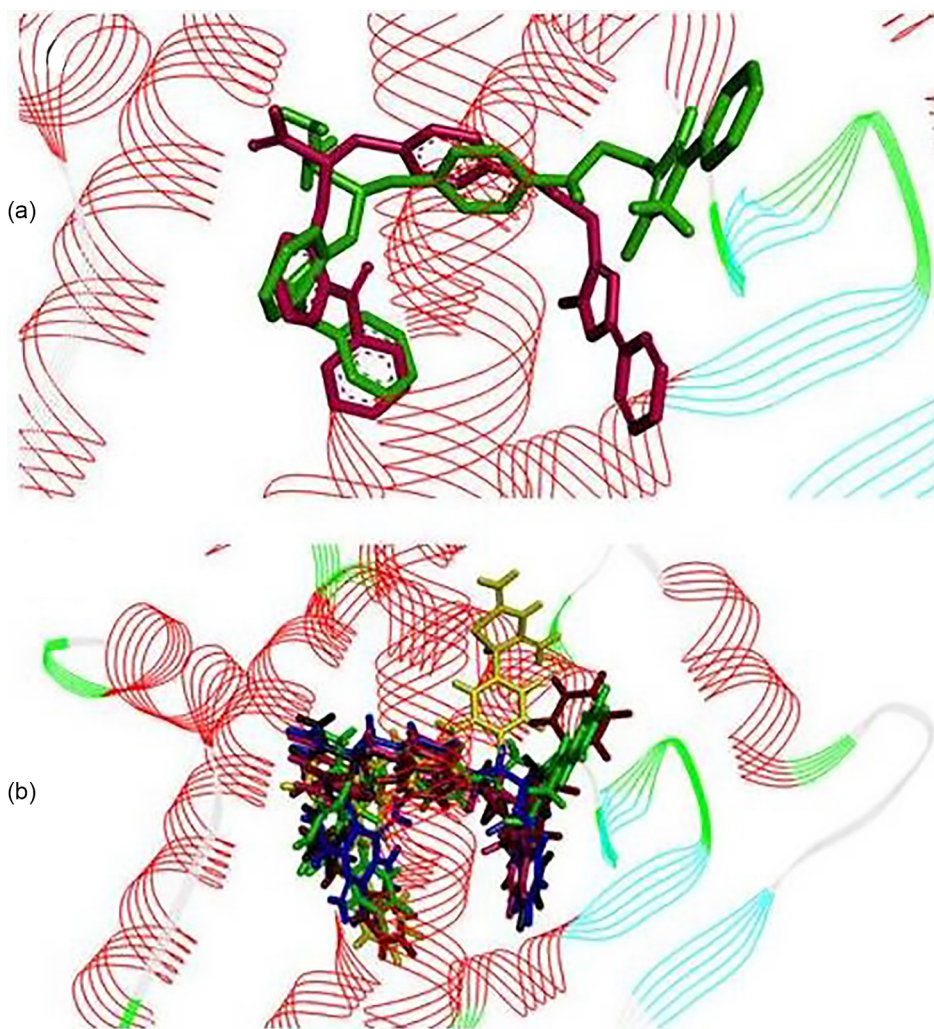


Figure 3. (a) Comparison between the crystallographic 1RDT molecule (red) and the best pose from GOLD docking software (green); (b) result of GOLD docking of selected Binding DB ligands and PPAR γ . The six best ligands are shown. 1RDT (green), CID77999 (pink), CID446642 (red), CID9827261 (yellow), CID10578809 (blue) and CID18944089 (black).

New proposed ligands obtained better GOLD score than crystallographic molecule

It is known that the hydrophobic tail of PPAR agonists may bind to the residues in the active site of the protein and the polar heads can interact with tyrosine residues producing activation effect. Such interactions give specificity to the molecule for the PPAR subtype, and changes in these regions may change this selectivity.¹⁵

Based on these reports and the pharmacophoric and conformational information previously obtained, we proposed seven new ligands for PPAR γ , maintaining the torsion of the molecule and pharmacophoric groups, and altering the polar head groups and hydrophobic tail (Figure 4a). Then, they were inserted in GOLD software in order to predict its conformation inside the binding site and docking score. The candidates were docked along with the crystallographic 1RDT molecule, also used in the

validation, to provide an internal control of the method. Candidate 1, candidate 2 and candidate 7 obtained the highest GOLD scores, 91.46, 70 and 96.19, respectively, while crystallographic molecule 1RDT obtained 85.61 (Supplementary Information section, see Table S2). The best poses are shown in the Figure 4b. The molecules follow the same folding pattern as they bypass the 278-294 helix and reach the space near the 339-349 loop with the 323-333 helix on the back, indicating that can also bind and activate PPAR γ . A closer look at the interactions between these 3 molecules and the protein are depicted in the Figure 4b.

Docking of candidates with PPAR α , PPAR δ and PPAR γ subtypes

In order to evaluate whether the changes made would present a higher binding affinity than the specific ligand for each PPAR subtypes, we docked each subtype, its

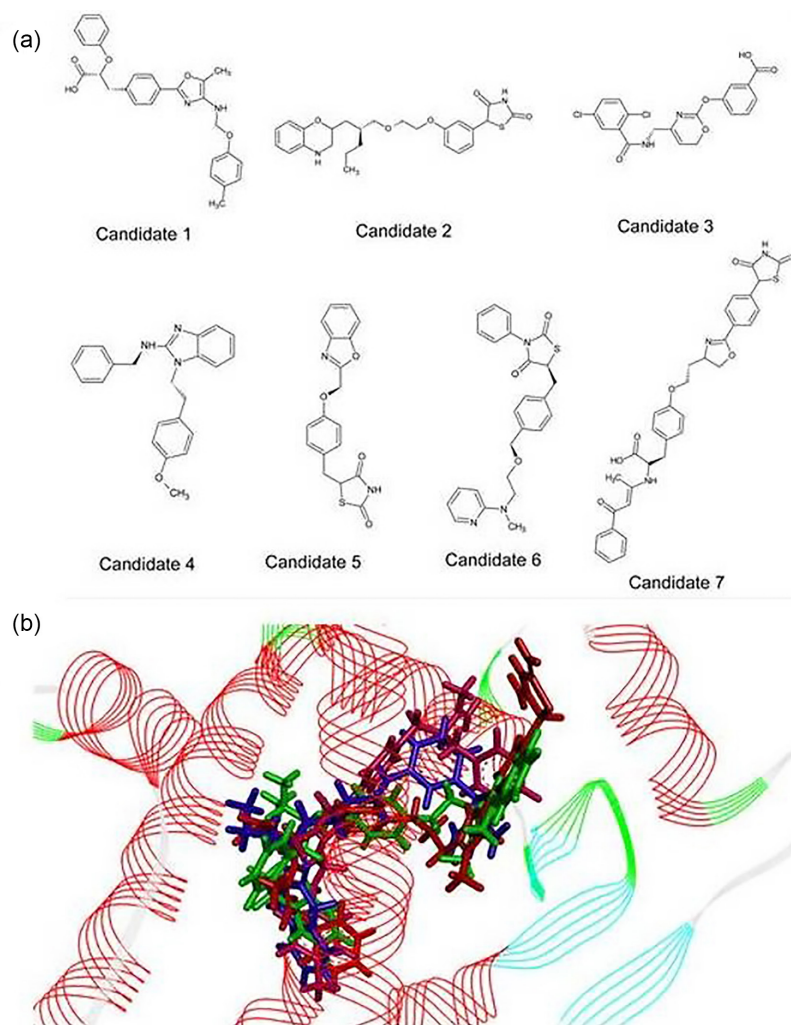


Figure 4. (a) Proposed ligands with changes in polar head and hydrophobic tail; (b) result of GOLD docking. Proposed ligands with higher GOLD score are shown with the best poses. IRDT (green), candidate 1 (pink), candidate 2 (blue) and candidate 7 (red).

specific ligand and candidates 1, 2 and 7 in AutoDock/Vina software. Autodock validation is shown in Figure 5. We observed that candidates 1 and 2 showed higher binding affinity to PPAR α than tesaglitazar (PDB 1I7I), a known agonist of this subtype, but candidate 7 showed lower affinity (Figure 6 and Supplementary Information section, see Table S3). The candidate 1 showed higher affinity for PPAR δ than the molecule TIPP204 (PDB 2ZNP) a ligand that was crystallographed with this receptor. However, candidates 2 and 7 showed lower affinity. For PPAR γ subtype, the three evaluated candidates had higher affinity than the agonist rosiglitazone (CID 77999), see Figure 6. We can also observe higher number of interactions of candidate 1 with the receptors than the specific ligands, corroborating the binding affinity predictions (Figure 6 and Table 1). With these data, we propose that the candidate 1 is capable of binding to three PPAR subtypes with greater binding affinity than their known activators.

Proposed molecules presents favorable pharmacokinetics and toxicity predictions

The candidates 1, 2 and 7 were submitted to the QikProp software in order to predict its pharmacokinetics. Candidate 1 presented only 1 Lipinski violation, on log P with a 6.3 value, a consequence of the high log P was a low aqueous solubility, log S of -7.6 , below the QikProp criteria (-6.5 to 0.5). The percentage of human oral absorption in gastrointestinal (GI) stood out with a 94% value, other absorption parameters such as Caco-2 permeability and Madin-Darby canine kidney (MDCK) permeability were considered in range for QikProp criteria. Candidate 1 presented number of stars of 2 which is in range to be considered a “drug-like” molecule (0-5, 0 being ideal). Candidate 2 presented a high Caco-2/MDCK permeability and percentage of human oral absorption in GI of 100%. No Lipinski violations was found but QikProp identified 10 possible metabolites for candidate 2 which is above the software range (1-8) and also presented 2

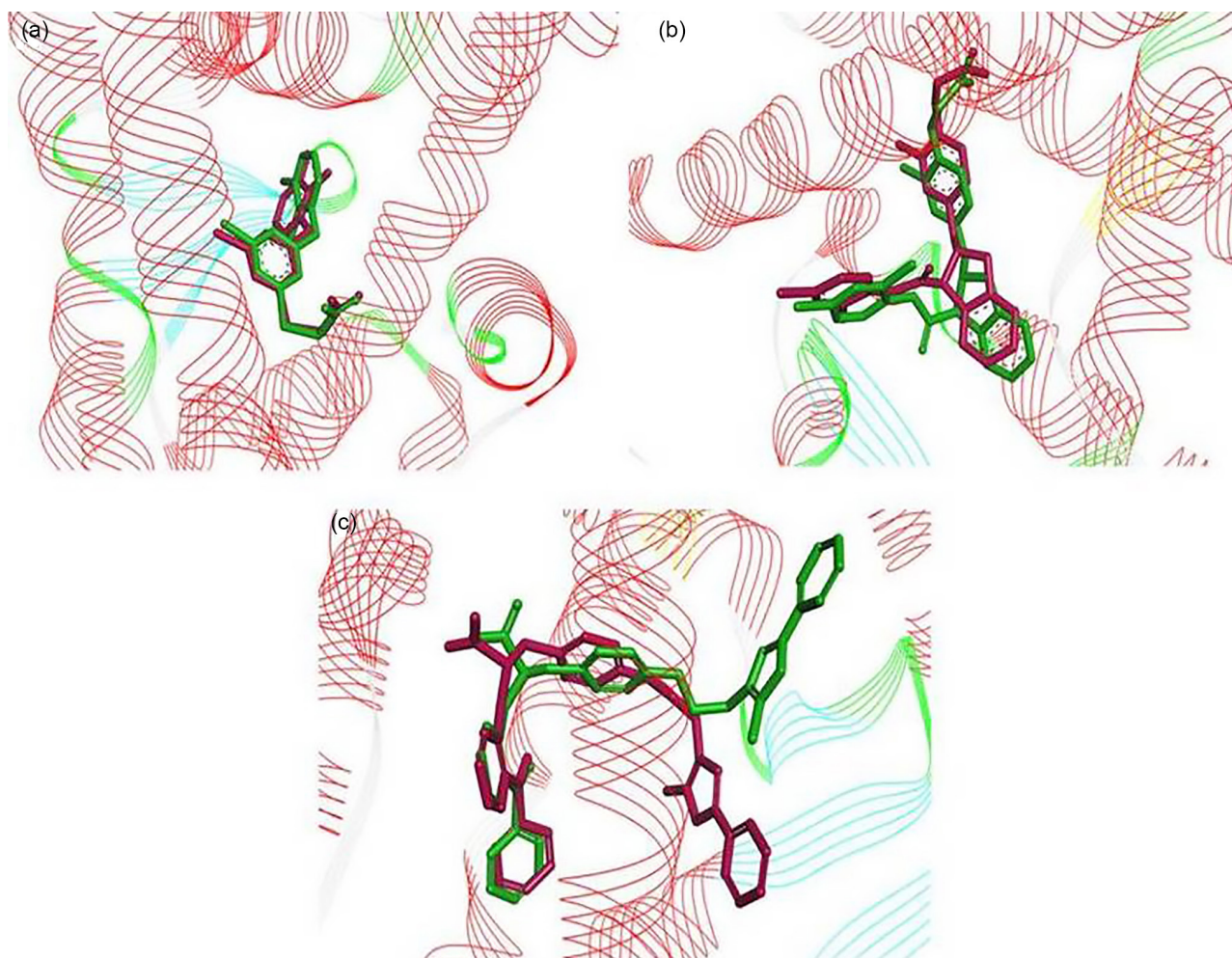


Figure 5. AutoDock validation of (a) PPAR α (PDB 4BCR); (b) PPAR δ (PDB 3OZ0); (c) PPAR γ (PDB 1RDT) with respective crystallographic molecules. Crystallographic molecules (red) and the best pose from AutoDock (green) are shown.

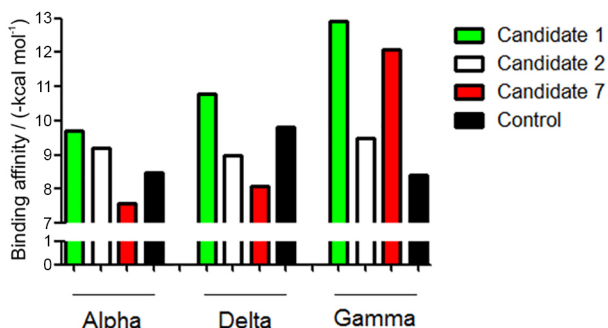


Figure 6. Binding affinity provided by AutoDock/Vina software of the best candidates and standard agonists. Ligand control for PPAR α , PPAR δ and PPAR γ were tesaglitazar, TIPP204 and rosiglitazone.

stars of drug likeliness. Another feature that stood out for candidate 2 is its similarity with other PPAR γ activator, the troglitazone (79.51% similarity). Candidate 7 also presented a low aqueous solubility -7.8 (-6.5 to 0.5), nine predicted metabolite (1-8) and 2 Lipinski violations. Its oral absorption (56%) was the lowest among the candidates and presented the number of stars of drug likeliness of 3.

Candidates 1, 2 and 7 were also submitted to Derek toxicity prediction software as another resource to choose a safer candidate to the synthesis. Candidate 1 presented the lowest toxicity between the candidates; the only output available in Derek was the ability to activate the peroxisome proliferation. Candidates 2 and 7 both present a thiazolidinedione group which is a known hepatotoxic group. However, there are thiazolidinediones currently in the market and this characteristic does not hinder the continuity of these candidates. The main issue is that the candidate 7 presented also genotoxicity due to the occurrence of a vinyl ketone group that is a considerable issue that should be taken into account.

Discussion

Molecular features

The PharmaGist analysis provided insightful information on the pharmacophoric group and other

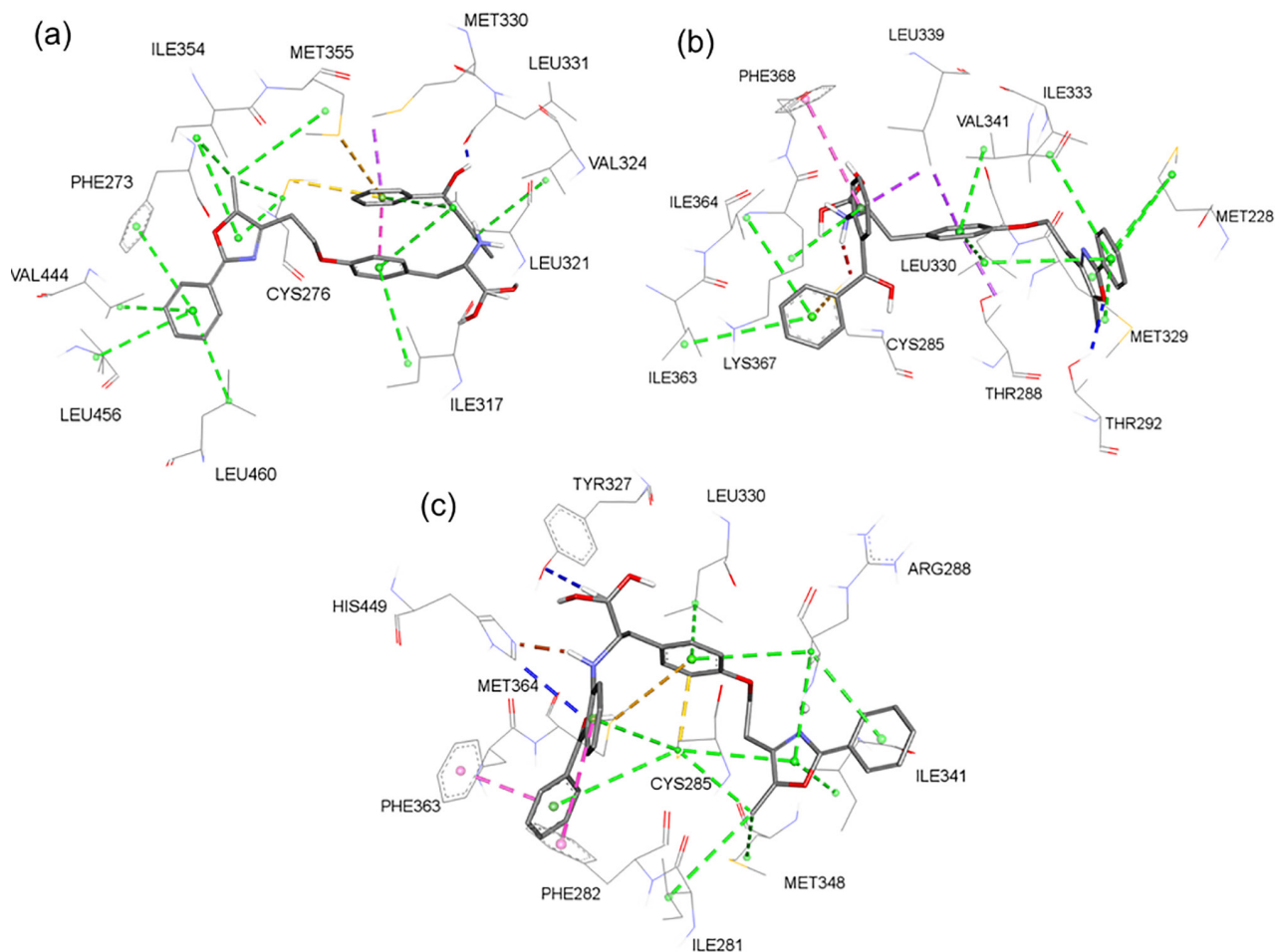


Figure 7. Interactions of candidate 1 with: (a) PPAR α ; (b) PPAR δ ; (c) PPAR γ . Green lines are hydrophobic interactions alkyl or Pi-alkyl. Orange lines are Pi-sulfur interactions. Blue lines are hydrogen bonds and pink lines are Pi-Pi interactions. Nominal interactions, aminoacids and distances can be seen in Table 1.

spatial features about the molecule folding. It can be seen in Figure 2 that a molecule intended to be active on this binding pocket should be able to fold around the alpha helix 278-294, where the pharmacophoric group will bind. Viewing the PharmaGist superposition output in DS Viewer we were able to observe that most of the test molecules have a folding characteristic that should be explored in drug candidates. The docking validation was accepted and the protein structures that interacted with the test molecules were similar to the ones found in a previous rosiglitazone interaction study which were His 323, His 449, Tyr 327, Tyr 473, Lys 367 and Ser 289.¹⁴ Following the 2 rings that form the pharmacophoric group, the folding of the molecules occurs through an aliphatic oxygen or nitrogen that provides an angle to the following chain. This pattern is repeated in the majority of the test molecules. These features which provided the interaction between the ligands and PPAR γ were maintained in the development of new molecules but polar head and hydrophobic tail varied, for the purpose of identifying molecules which interact with

the three PPAR subtypes tested. Thus, we detected three candidates that maintained good binding affinity to PPAR γ , and the candidate 1 also shows binding affinity to PPAR α and PPAR δ .

Candidates outcome

The GOLD docking was used to select the most viable candidates among the proposals. In this test, candidates 1 and 7 stood out scoring above 90 in the test, even more than the crystallographic molecule 1RDT which scored around 85. Candidate 2 obtained 70 GOLD score and was selected too. When the binding affinity of selected candidates was compared with rosiglitazone, all of them obtained a better score, indicating that they maintained good binding affinity to PPAR γ . Comparing the binding affinity of these candidates with tesaglitazar (PPAR α agonist) and TIPP204 (PPAR δ ligand), the candidate 1 stood out presenting a higher score than all of these selective ligands. However, the candidate 2 showed an affinity better than the controls

Table 1. Interactions between candidate 1 and specific ligands with PPARs

Molecule	Aminoacid	Distance / Å	Type
Candidate 1 vs. PPAR α	LEU331	1.87	hydrogen bond
	MET330	3.73	pi-sigma
	CYS276	4.36	pi-sulfur
	MET355	5.18	pi-sulfur
	VAL444, LEU456, LEU460, CYS276, ILE354, MET355, PHE273, VAL324, LEU321, ILE317, CYS276, ILE354, CYS276	3.49-5.44	alkyl
117I vs. PPAR α	HIS440	2.08	hydrogen bond
	HIS440	3.32	hydrogen bond
	SER280	2.95	unf acceptor-acceptor
	THR279	3.86	pi-sigma
	CYS276, LEU321, VAL324	4.54-5.13	pi-alkyl
Candidate 1 vs. PPAR δ	THR292	2.44	hydrogen bond
	CYS285	2.29	unf donor-donor
	THR288	3.45	pi-sigma
	LEU339	3.99	pi-sigma
	LEU339	3.39	pi-sigma
	CYS285	3.87	pi-sulfur
	PHE368	5.03	pi-pi t-shaped
	MET228, MET329, LEU330, ILE333, LYS367, ILE363, ILE364, LEU330, VAL341, MET228	4.70-5.38	alkyl
	TIPP204 vs. PPAR δ	ARG284	3.37
LEU330		3.43	pi-sigma
VAL341		3.96	pi-sigma
LEU255, VAL281, VAL348, MET453, LEU469		3.74-5.11	alkyl
CYS285, LYS367, VAL281, ARG284, CYS285, VAL348		4.83-5.41	pi-alkyl
Candidate 1 vs. PPAR γ	HIS449	2.16	hydrogen bond
	HIS449	3.54	carbon hydrogen bond
	TYR327	2.98	carbon hydrogen bond
	CYS285	3.97	pi-sulfur
	MET364	5.42	pi-sulfur
	PHE363	3.91	pi-pi stacked
	PHE282	4.94	pi-pi t-shaped
	ARG288, ILE281, CYS285, MET348	4.33-5.01	alkyl
	CYS285, CYS285, ARG288, LEU330, CYS285, ARG288, ILE341	4.16-5.23	pi-alkyl
Rosiglitazone vs. PPAR γ	SER289	3.65	carbon hydrogen bond
	CYS285	3.64	carbon hydrogen bond
	TYR327	3.63	carbon hydrogen bond
	HIS449	3.67	carbon hydrogen bond
	CYS285	3.65	pi-sigma
	CYS285	4.25	pi-sulfur
	MET364	5.49	pi-sulfur
	PHE360	5.80	pi-sulfur
	PHE282	4.42	pi-pi stacked
	PHE363	5.41	pi-pi t-shaped
	CYS285, LEU453	5.01-5.31	pi-alkyl

for PPAR α and PPAR γ , therefore it is also a promising candidate. Candidate 7 presented a high and selective activity to PPAR γ , which is an unwanted feature due to the toxicity that this selective interaction may provide.

Pharmacokinetics and toxicity issues are responsible for 50% of a molecule discontinuity and these studies should be assessed early in the drug development in order to avoid unnecessary investment.³¹ The Derek software did not found important toxicity for the candidate 1. Candidate 2 showed an expected toxicity due to its thiazolidinedione group which is known to cause hepatotoxicity, however it does not hinder its continuity forward to synthesis and *in vitro/in vivo* tests to determine the extension of this toxicity as the thiazolidinedione group is also present in molecules that have already reached the market.^{32,33}

Candidate 7 not only presented the thiazolidinedione known toxicity but also chromosome toxicity due to the vinyl ketone group, which reacts with guanine in DNA, causing genotoxic effects.³⁴ This toxicity profile allied with the selective and strong activation of PPAR γ make this candidate unviable for further tests.

The pharmacokinetics of candidates 1 and 2 presented good oral absorption and 2 stars on QikProp criteria to describe drug likeliness, comparing both these candidates, candidate 2 stood out with a better aqueous solubility and no Lipinski's rule flaw, however it presents many routes of metabolism with 10 predicted metabolites, which may lead to variability on toxicity/activity of these metabolites and also, many metabolic pathways may lead to a high clearance and therefore low half-life which may limit its dose regimen. Candidate 7 presented the most undesirable pharmacokinetics characteristics presenting low aqueous solubility, 2 Lipinski flaws and 9 possible metabolites. It also presented 56% oral absorption, lower than candidates 1 and 2 (94 and 100%, respectively).

A new lead molecule

There is a tendency for the treatment of metabolic disease to develop drug candidates that activate the 3 PPARs in order to avoid the adverse effects observed in single or dual activators, like the glitazars that had a few analogs such as muraglitazar, tesaglitazar, ragaglitazar, TAK559 and KRP297 that stopped in clinical trials by FDA due to side effects, mainly hepatotoxicity.^{35,36}

The glitazars, activators of PPAR α and PPAR γ have also been researched for the activation of PPAR δ , as happened recently with chiglitazar³⁷ that demonstrated low toxicity compared with selective PPAR γ or dual agonists and was able to advance to phase 3 in clinical trials. Besides chiglitazar, LYSO-07 designed initially as a PPAR γ agonist

also presented PPAR α and PPAR δ activation, this PPAR pan agonism boosted its research.^{38,39} Other molecules like ZBH and CNX-013-B2 also were researched for a PPAR pan agonism which is considered by the researchers a characteristic that may represent a promising adverse effect profile in *in vivo* studies.^{40,41}

Candidate 1 herein presented is a molecule similar to LY465608, used as a lead structure in PPAR pan agonists design. However, it was halted from clinical trials due to hepatotoxicity presented in animal models.^{35,42-44} Despite the structural similarity, candidate 1 did not show predicted hepatotoxicity in Derek software and, just like previous drug candidates leaded by LY465608,³⁵ we obtained a molecule with higher affinity to the receptors than their specific agonists, therefore the candidate 1 demonstrates potential to figure as an innovative drug candidate to either lead the proposals of new PPAR pan ligands or even be synthesized and go further to *in vitro/in vivo* studies.

Conclusions

In conclusion, candidate 1 showed higher binding affinity than specific ligands for PPAR $\alpha/\gamma/\delta$, favorable pharmacokinetic and toxicological parameters, leading this molecule to figure as an efficient drug candidate that can control blood sugar, decrease free fatty acid, and low-density lipoprotein concentration, increase high-density lipoprotein concentration, reduce cardiovascular diseases without the adverse effects from PPAR γ selective agonists. Due to the rise of PPAR pan agonists, the candidate 1 represents a new lead to develop molecules with this promising characteristic and even advance to *in vitro/in vivo* studies.

Supplementary Information

PharmaGist server (<http://bioinfo3d.cs.tau.ac.il/pharma/index.html>) were used for pharmacophore prediction. The GOLD Score of candidates, crystallographic molecule 1RDT and PPAR γ ligands docked with PPAR γ receptor, binding affinity of candidates 1, 2 and 7 and specific PPAR ligands was assessed with AutoDock/Vina software and calculated physicochemical properties are available free of charge at <http://jbcbs.s bq.org.br> as PDF file.

Acknowledgments

We gratefully acknowledge the financial support provided by the Brazilian Agency National Council of Scientific and Technological Development (CNPq) and São Paulo Research Foundation (FAPESP).

References

1. Pourcet, B.; Fruchart, J. C.; Staels, B.; Glineur, C.; *Expert Opin. Emerging Drugs* **2006**, *11*, 379.
2. Barrera, G.; Toaldo, C.; Pizzimenti, S.; Cerbone, A.; Pettazzoni, P.; Dianzani, M. U.; Ferretti, C.; *PPAR Res.* **2008**, 524.
3. Kidani, Y.; Bensinger, S.; *Immunol Rev.* **2012**, *249*, 72.
4. Tontonoz, P.; Hu, E.; Spiegelman, B. M.; *Cell* **1994**, *79*, 56.
5. Schoonjans, K.; Watanabe, M.; Suzuki, H.; Mahfoudi, A.; Krey, G.; Wahli, W.; Grimaldi, P.; Staels, B.; Yamamoto, T.; Auwerx, J.; *J. Biol. Chem.* **1995**, *270*, 19269.
6. Schoonjans, K.; Staels, B.; Auwerx, J.; *J. Lipid Res.* **1996**, *37*, 907.
7. Sfeir, Z.; Ibrahimi, A.; Amri, E.; Grimaldi, P.; Abumrad, N.; *Prostaglandins, Leukotrienes Essent. Fatty Acids* **1997**, *57*, 17.
8. Soccio, R. E.; Chen, E. R.; Lazar, M. A.; *Cell Metab.* **2014**, *20*, 573.
9. Mangelsdorf, D. J.; Borgmeyer, U.; Heyman, R. A.; Zhou, J. Y.; Ong, E. S.; Oro, A. E.; Kakizuka, A.; Evans, R. M.; *Genes Dev.* **1992**, *6*, 329.
10. Chao, L.; Marcus, S. B.; Mason, M. M.; Moitra, J.; Vinson, C.; Arioglu, E.; Gavriloiva, O.; Reitman, M. L.; *J. Clin. Invest.* **2000**, *106*, 1221.
11. Graham, D. J.; Ouellet-Hellstrom, R.; MaCurdy, T. E.; Ali, F.; Sholley, C.; Worrall, C.; Kelman, J. A.; *JAMA* **2010**, *304*, 411.
12. MacDonald, M. R.; Petrie, M. C.; Home, P. D.; Komajda, M.; Jones, N. P.; Beck-Nielsen, H.; Gomis, R.; Hanefeld, M.; Pocock, S. J.; Curtis, P. S.; McMurray, J. J.; *Diabetes Care* **2011**, *34*, 1394.
13. Pignone, M.; *Clin. Diabetes* **2007**, *25*, 123.
14. Silva, F. M. C.; dos Santos, J. C.; Campos, J. L.; Mafud, A. C.; Polikarpov, I.; Figueira, A. C.; Nascimento, A. S.; *Bioorg. Med. Chem. Lett.* **2013**, *23*, 5795.
15. Su, J. H.; Chang, C.; Xiang, Q.; Zhou, Z. W.; Luo, R.; Yang, L.; He, Z. X.; Yang, H. T.; Li, J.; Bei, Y.; Xu, J. M.; Zhang, M. J.; Zhang, Q. H.; Su, Z. J.; Huang, Y. D.; Pang, J. Y.; Zhou, S. F.; *Drug Des., Dev. Ther.* **2014**, *8*, 2255.
16. Braissant, O.; Fougelle, F.; Scotto, C.; Dauça, M.; Wahli, W.; *Endocrinology* **1996**, *137*, 354.
17. Oliver, W. R.; Shenk, J. L.; Snaith, M. R.; Russell, C. S.; Plunket, K. D.; Bodkin, N. L.; Lewis, M. C.; Winegar, D. A.; Sznajdman, M. L.; Lambert, M. H.; Xu, H. E.; Sternbach, D. D.; Kliewer, S. A.; Hansen, B. C.; Willson, T. M.; *Proc. Natl. Acad. Sci. U.S.A.* **2001**, *98*, 5306.
18. Wang, Y. X.; Zhang, C. L.; Yu, R. T.; Cho, H. K.; Nelson, M. C.; Bayuga-Ocampo, C. R.; Ham, J.; Kang, H.; Evans, R. M.; *PLoS Biol.* **2004**, *2*, 294.
19. Nevin, D. K.; Peters, M. B.; Carta, G.; Fayne, D.; Lloyd, D. G.; *J. Med. Chem.* **2012**, *55*, 4978.
20. Harrington, W. W.; Britt, C. S.; Wilson, J. G.; Milliken, N. O.; Binz, J. G.; Lobe, D. C.; Oliver, W. R.; Lewis, M. C.; Ignar, D. M.; *PPAR Res.* **2007**, *2007*, 97125.
21. Wickens, P.; Zhang, C.; Ma, X.; Zhao, Q.; Amatruda, J.; Bullock, W.; Burns, M.; Cantin, L. D.; Chuang, C. Y.; Claus, T.; Dai, M.; Dela Cruz, F.; Dickson, D.; Ehrgott, F. J.; Fan, D.; Heald, S.; Hentemann, M.; Iwuagwu, C. I.; Johnson, J. S.; Kumarasinghe, E.; Ladner, D.; Lavoie, R.; Liang, S.; Livingston, J. N.; Lowe, D.; Magnuson, S.; Mannelly, G.; Mugge, I.; Ogutu, H.; Pleasic-Williams, S.; Schoenleber, R. W.; Shapiro, J.; Shelekhin, T.; Sweet, L.; Town, C.; Tsutsumi, M.; *Bioorg. Med. Chem. Lett.* **2007**, *17*, 4369.
22. Batista, F. A.; Trivella, D. B.; Bernardes, A.; Gratieri, J.; Oliveira, P. S.; Figueira, A. C.; Webb, P.; Polikarpov, I.; *PLoS One* **2012**, *7*, 33643.
23. Rubenstrunk, A.; Hanf, R.; Hum, D. W.; Fruchart, J. C.; Staels, B.; *Biochim. Biophys. Acta* **2007**, *1771*, 1065.
24. Van de Waterbeemd, H.; Gifford, E.; *Nat. Rev. Drug Discov.* **2003**, *2*, 192.
25. Tolman, K. G.; Chandramouli, J.; *Clin. Liver Dis.* **2003**, *7*, 369.
26. Scheen, A. J.; *Drug Saf.* **2001**, *24*, 873.
27. Eder, E.; Hoffman, C.; Deininger, C.; *Chem. Res. Toxicol.* **1991**, *4*, 50.
28. Zhang, L. S.; Wang, S. Q.; Xu, W. R.; Wang, R. L.; Wang, J. F.; *PLoS One* **2012**, *7*, 48453.
29. Oyama, T.; Toyota, K.; Waku, T.; Hirakawa, Y.; Nagasawa, N.; Kasuga, J. I.; Hashimoto, Y.; Miyachi, H.; Morikawa, K.; *Acta Crystallogr., Sect. D: Biol. Crystallogr.* **2009**, *8*, 786.
30. Morris, G. M.; Huey, R.; Lindstrom, W.; Sanner, M. F.; Belew, R. K.; Goodsell, D. S.; Olson, A. J.; *J. Comput. Chem.* **2009**, *16*, 2785.
31. Hage-Melim, L. I. S.; Santos, C. B. R.; Poiani, J. G.; Vaidergom, M. M.; Manzolli, E. S.; Silva, C. H. T. P.; *Curr. Bioact. Compd.* **2014**, *10*, 147.
32. Tolman, K. G.; Chandramouli, J.; *Clin. Liver Dis.* **2003**, *7*, 369.
33. Scheen, A. J.; *Drug Saf.* **2001**, *24*, 873.
34. Eder, E.; Hoffman, C.; Deininger, C.; *Chem. Res. Toxicol.* **1991**, *4*, 50.
35. Zhang, L. S.; Wang, S. Q.; Xu, W. R.; Wang, R. L.; Wang, J. F.; *PLoS One* **2012**, *7*, 48453.
36. Conlon, D.; *Br. J. Diabetes Vasc. Dis.* **2006**, *6*, 135.
37. He, B. K.; Ning, Z. Q.; Li, Z. B.; Shan, S.; Pan, D. S.; Ko, B. C.; Li, P. P.; Shen, Z. F.; Dou, G. F.; Zhang, B. L.; Lu, X. P.; Gao, Y.; *Res.* **2012**, *2012*, 546.
38. Garcia, G. M.; Oliveira, L. T.; Ida, R. P.; de Lima, M. C.; Vilela, J. M.; Andrade, M. S.; Abdalla, D. S.; Mosqueira, V. C.; *J. Control. Release* **2015**, *209*, 207.
39. Santin, J. R.; Daufenback Machado, I.; Rodrigues, S. F.; Teixeira, S.; Muscará, M. N.; Lins Galdino, S.; Pitta, I. R.; Farsky, S. H.; *PLoS One* **2013**, *8*, 76894.
40. Chen, W.; Fan, S.; Xie, X.; Xue, N.; Jin, X.; Wang, L.; *PLoS One* **2014**, *9*, 96056.

41. Sadasivuni, M. K.; Reddy, B. M.; Singh, J.; Anup, M. O.; Sunil, V.; Lakshmi, M. N.; Yogeshwari, S.; Chacko, S. K.; Pooja, T. L.; Dandu, A.; Harish, C.; Gopala, A. S.; Pratibha, S.; Naveenkumar, B. S.; Pallavi, P. M.; Verma, M. K.; Moolemath, Y.; Somesh, B. P.; Venkataranganna, M. V.; Jagannath, M. R.; *Diabetol. Metab. Syndr.* **2014**, *6*, 83.
42. Guo, Y.; Jolly, R. A.; Halstead, B. W.; Baker, T. K.; Stutz, J. P.; Huffman, M.; Calley, J. N.; West, A.; Gao, H.; Searfoss, G. H.; Li, S.; Irizarry, A. R.; Qian, H. R.; Stevens, J. L.; Ryan, T. P.; *Toxicol. Sci.* **2007**, *96*, 294.
43. Vieira, J.; Braga, F.; Lobato, C.; Santos, C.; Costa, J.; Bittencourt, J.; Brasil, D.; Silva, J.; Hage-Melim, L.; Macêdo, W.; Carvalho, J.; Santos, C.; *Molecules* **2014**, *19*, 10670.
44. Santos, C. B. R.; Lobato, C. C.; Braga, F. S.; Costa, J. S.; Favacho, H. A. S.; Carvalho, J. C. T.; Macedo, W. J. C.; Brasil, D. S. B.; Silva, C. H. T. P.; Hage-Melim, L. I. S.; *Curr. Pharm. Des.* **2015**, *21*, 4112.

Submitted: December 4, 2015

Published online: February 11, 2016

FAPESP has sponsored the publication of this article.